Available online at www.sciencedirect.com
SCIENCE DIRECT
ELSEVIER
Ocean Engineering 33 (2006) 382–403
OCEAN ENGINEERING
www.elsevier.com/locate/oceaneng

Effects of T-shape groin parameters on beach accretion

İsmail Hakkı Özölçer[a,*], Murat İhsan Kömürcü[b], Ali Remzi Birben[c], Ömer Yüksek[d], Servet Karasu[e]

[a]*Civil Engineering Department, Zonguldak Karaelmas University, 67100 Zonguldak, Turkey*
[b]*Turkish Maritime Organization, Inc., Trabzon, Turkey*
[c]*AKYAPI Engineering, 34670 İkitelli, İstanbul, Turkey*
[d]*Civil Engineering Department, Karadeniz Technical University, 61080 Trabzon, Turkey*
[e]*Vocational School, Karadeniz Technical University, 53100 Rize, Turkey*

Received 15 November 2004; accepted 20 April 2005
Available online 11 August 2005

Abstract

The effects of various groin parameters (length, head length and opening) and wave parameters (wave height, wave period and wave angle) on the accretion of the area protected by T-shape groins are studied in a physical model. The model studies are performed using regular waves in a basin. A numerical model which depends primarily on a CERC model is employed to examine the effects of some of the above parameters. Good agreement is found in the results of physical and numerical models. The results of a numerical model are compared with field data obtained by deep sounding measurements at Of coasts, Trabzon Province, Turkey. The finding from this study may be employed in designing T-shape groins.
© 2005 Elsevier Ltd. All rights reserved.

Keywords: Groins; Shore protection; Sediment transport; Accretion parameter; Numerical model; Field data

1. Introduction

Historically (say, for thousand of years), a coastal region, without any structure, could be in equilibrium from the sediment regime. A seasonal sediment transport

* Corresponding author. Fax: +90 372 257 4023.
E-mail addresses: ozolcer@hotmail.com (İ.H. Özölçer), ozolcer@karaelmas.edu.tr (İ.H. Özölçer).

0029-8018/$ - see front matter © 2005 Elsevier Ltd. All rights reserved.
doi:10.1016/j.oceaneng.2005.04.018

depending on dominant wave conditions and directions may be varying from one region to another. The net sediment transport is defined as the summation of cross-shore and long shore transport $Q_N = Q_{CR} + Q_{LR}$, where the cross-shore transport consists of offshore transport, Q_{off}, and onshore, Q_{on}, i.e., $Q_{CR} = Q_{off} + Q_{on}$. Long shore transport has components directed to the left, Q_L, and to the right, Q_R, leading to net transport $Q_{LR} = Q_L + Q_R$; where Q_L is taken as negative. Balance in sediment budget is disrupted by the construction as a coastal structure, dredging of sediment for navigation channel, etc.

A groin is a shore protection structure designed to trap littoral drift and, to some extent, the cross-shore sediment for creating a protective beach, retarding erosion of an existing beach, or preventing long shore drift from reaching some downdrift point, such as a harbor or inlet. Groins are narrow structures of variable lengths and heights and are usually constructed in perpendicular to shoreline. Groins can be constructed as a single structure or in series (groin field).

Several investigations have been conducted in the past to study the effect of groin parameters on beach accretion. Some of the most important studies and their conclusions are summarized as follows.

Press (1962) performed physical model studies on straight groins and recommended some criteria about the accretion amount and groin opening.

Price and Tomlinson (1968) conducted a study on the effects of groins on stable beaches and studied the coastal changes for various groin parameters, using a three-dimensional physical model. The effect of the groins on the beach was similar for the different wave angle ($\alpha = 20, 5°$) and for the fixed groin spacing.

Brampton and Goldberg (1991a,b) studied the effects of groins on shingle beaches on the beach evolution, using a three-dimensional physical model. They studied a shore with three groins, and after 10 yearly observations they found that the accretion at the updrift side of groins was equal to the erosion at the downdrift side.

Hanson and Kraus (1991) experimentally studied the effects of a series of three groins on shore evolution and proposed a numerical model (GENESIS) and concluded that this model was in agreement with the findings of the physical model.

Moutzouris (1992) studied the erosion problem derived from the construction a fishery harbor. At the end of a series of physical models, he proposed the construction of six groins and observed that, field data obtained after the construction of the groins were in a good agreement with the physical model results.

Kraus et al. (1994), who carried out physical model studies on groin parameters, proposed that groin length be equal to groin opening.

Güngördü and Otay (1997) proposed a numerical model to calculate the shoreline changes in the vicinity of a groin employing only long shore sediment transport and compared their model with field data obtained from four yearly observations.

Leont'yev (1997), in this study, the proposed numerical simulates the short-term temporal changes in shoreline position due to a structure interrupting the long shore sediment flux. The impacts of the groin-type construction and under water trench of arbitrary orientation relative to the shore are investigated and he tested the model against the laboratory data of Baidei et al.

In this study, the effects of various groin and wave parameters on the accretion of the area protected by T groins are studied both by physical and numerical models. The results of a numerical model are compared with field data that were obtained by deep sounding measurements at Of Coasts, Trabzon Province, Turkey. The dominant wave direction of the location varies from NW to N, causing net littoral transport from west to east (Yüksek, 1995; Yüksek et al., 1999). The developed numerical model computes the evolution of bed contours depending on both long shore and cross-shore sediment transport discharges.

2. Laboratory studies

2.1. Model basin

Physical model studies were performed at the Karadeniz Technical University (K.T.U.), using a wave basin with $30\times12\times1.5$ m. An undistorted model scale of 1/75 was selected by taking into account the dimensions of the basin and wise an average groin. The slope of the model bed was $m=1/25$ and the bed material was fine sand $d_{50}=0.16$ mm. Reproducing the movement of sediment in small-scale models is very difficult, and scaling relations have not been developed to accurately measure the quantitative movement of sediment. Several research projects, in this area, are being conducted. Thus, it is not possible to determine which material, in nature, would correspond to the fine sand used. However in the laboratory, the bed material was easily transported by waves, and it was assumed that its qualitative movement was representative of the prototype.

In the model basin (Fig. 1), there were a wave-generator system, a speed control system, and a wave-height measurement system for the generation and measurement of waves. Monochromatic wave height was controlled by a screwed handle and wave period by a speed control. An electronic wave gauge was used to measure the wave heights in the basin as follows: An electronic bar was into the basin at some 5 m from the wave paddle and 20 cm below the still water level. A constant current ($I=12$ A) was loaded to the bar. As water levels over the bar were changed by the waves, the resistance of the water over the bar (R), and consequently the voltages, changed ($V=R^*I$, I was constant). These voltage changes were recorded on a chart. The relationship between voltage and water level changes (waves) was determined by calibration before the experiments. Wave heights were calculated using this calibration. A chronometer measured wave periods.

2.2. Performing experiments

The bed material (sand) was spread over the basin bed. The waves, affecting littoral sediment transport, were angle α to the shoreline. To represent these waves, taking into consideration the restrictions imposed by the basin dimensions, a maximum wave angle about $\alpha_0=30^\circ$ was chosen for the deep-water waves.

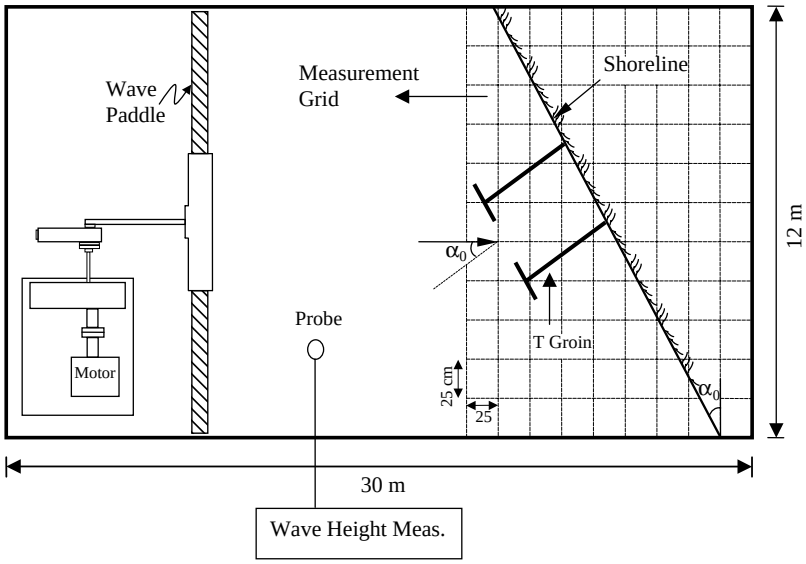


Fig. 1. Experimental set-up in a wave basin.

The groins were constructed of stone blocks surrounded by sheet irons. The sheet irons were sunk into the bed in order to make them impermeable to both the waves and sediment.

The model zone was divided by 25×25 cm grids. Within each grid, elevations of the sandy surface in the basin, before and after an experiment (h_1 and h_2, respectively), were measured using a ruler and the accumulation height was determined by Δh (h_2–h_1). Preliminary experiments showed that a testing period of $t=240$ min (35 h in prototype) was sufficient; at the end of this period, the shoreline reached an equilibrium.

2.3. Tested parameters

The tested groin parameters were groin length (L_X), head length (L_B) and spacing between successive groins (L_G) (Fig. 2). All of the tested groin and wave parameters are given in Table 1.

3. Analysis of experimental results

Experimental data are analyzed using three groin parameters, groin length (L_X), head length (L_B) and spacing between successive groins (L_G), which were identified from previous study (Özölçer, 1998):

A dimensionless accretion parameter is defined as follows (Fig. 3);

$$R = \frac{\sum D \times A_s}{A_G \times H} \tag{1}$$

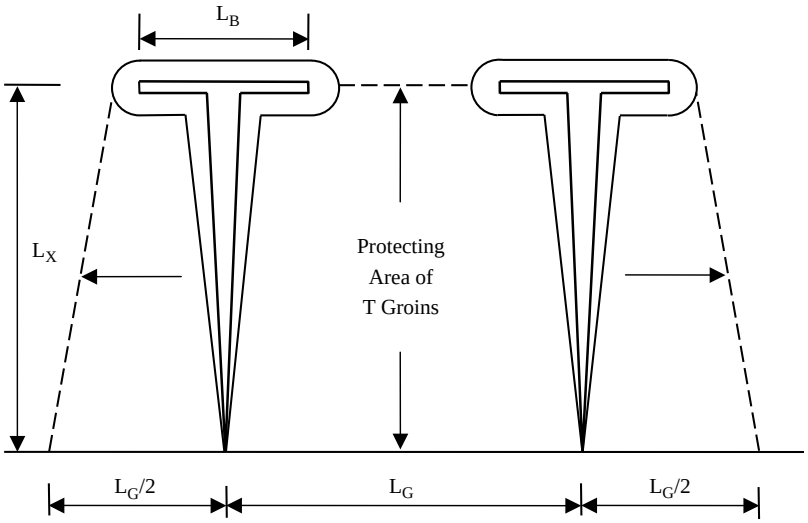


Fig. 2. Groin parameters and protecting area.

where D is the total accretion height within the groin area; A_s is the area of a square in the measuring grid system (625 cm^2); A_G is the total area protected by groins (groin protection area) and H is wave height.

The total area protected by groin is calculated several geometrical dimensions of the groin:

$$A_G = \frac{\left[L_G + \frac{L_B}{2} + \frac{L_B}{2} + L_G + \frac{L_G}{2} + \frac{L_G}{2}\right] \times L_X}{2} = \frac{(L_B + 3 \times L_G) \times L_X}{2} \tag{2}$$

If there were a total of n measuring points within each of the square of 25×25, the total area of A_G become:

$$A_G = n \times 25 \times 25 = 625 \times n = n \times A_S \tag{3}$$

Inserting Eq. (3) into Eq. (1), given

$$R = \frac{\sum D \times A_S}{n \times A_S \times H} = \frac{D_1 \times (25 \times 25) + D_2 \times (25 \times 25) + \cdots + D_n \times (25 \times 25)}{n \times A_S \times H}$$

$$= \frac{D_1 \times A_S + D_2 \times A_S + \cdots + D_n \times A_S}{n \times A_S \times H} = \frac{A_S \times (D_1 + D_2 + \cdots + D_n)}{n \times A_S \times H}$$

$$= \frac{\sum D}{n \times H} \tag{4}$$

All of the R values obtaining from tests is given in Table 1.

Table 1
Tested groin parameters

Test no	m	α (°)	T (s)	H (cm)	H/L	L_X (cm)	L_G (cm)	L_B (cm)	R
1	1/25	30	0.866	3.33	0.028	66.67	66.67	33.33	0.064
2	1/25	30	0.866	3.33	0.028	66.67	80.00	33.33	0.083
3	1/25	30	0.866	3.33	0.028	66.67	113.33	33.33	0.096
4	1/25	30	0.866	3.33	0.028	66.67	133.33	33.33	0.114
5	1/25	30	0.866	3.33	0.028	66.67	146.67	33.33	0.105
6	1/25	30	0.866	3.33	0.028	66.67	180.00	33.33	0.078
7	1/25	30	0.866	3.33	0.028	66.67	193.33	33.33	0.070
8	1/25	30	0.866	3.33	0.028	100.0	130.00	20.00	0.136
9	1/25	30	0.866	3.33	0.028	100.0	200.00	20.00	0.130
10	1/25	30	0.866	3.33	0.028	100.0	230.00	20.00	0.122
11	1/25	30	0.866	3.33	0.028	100.0	110.00	30.00	0.159
12	1/25	30	0.866	3.33	0.028	100.0	130.00	30.00	0.154
13	1/25	30	0.866	3.33	0.028	100.0	150.00	30.00	0.161
14	1/25	30	0.866	3.33	0.028	100.0	170.00	30.00	0.150
15	1/25	30	0.866	3.33	0.028	100.0	200.00	30.00	0.138
16	1/25	30	0.866	3.33	0.028	100.0	230.00	30.00	0.142
17	1/25	30	0.866	3.33	0.028	100.0	250.00	30.00	0.139
18	1/25	30	0.866	3.33	0.028	100.0	130.00	40.00	0.156
19	1/25	30	0.866	3.33	0.028	100.0	170.00	40.00	0.144
20	1/25	30	0.866	3.33	0.028	100.0	200.00	40.00	0.144
21	1/25	30	0.866	3.33	0.028	100.0	230.00	40.00	0.130
22	1/25	30	0.866	3.33	0.028	100.0	100.00	50.00	0.089
23	1/25	30	0.866	3.33	0.028	100.0	110.00	50.00	0.094
24	1/25	30	0.866	3.33	0.028	100.0	130.00	50.00	0.129
25	1/25	30	0.866	3.33	0.028	100.0	160.00	50.00	0.108
26	1/25	30	0.866	3.33	0.028	100.0	170.00	50.00	0.138
27	1/25	30	0.866	3.33	0.028	100.0	200.00	50.00	0.132
28	1/25	30	0.866	3.33	0.028	100.0	210.00	50.00	0.108
29	1/25	30	0.866	3.33	0.028	100.0	230.00	50.00	0.124
30	1/25	30	0.866	3.33	0.028	100.0	260.00	50.00	0.108
31	1/25	30	0.866	3.33	0.028	100.0	290.00	50.00	0.089
32	1/25	30	0.866	3.33	0.028	100.0	130.00	60.00	0.160
33	1/25	30	0.866	3.33	0.028	100.0	170.00	60.00	0.144
34	1/25	30	0.866	3.33	0.028	100.0	200.00	60.00	0.148
35	1/25	30	0.866	3.33	0.028	100.0	230.00	60.00	0.136
36	1/25	30	0.866	3.33	0.028	100.0	100.00	70.00	0.163
37	1/25	30	0.866	3.33	0.028	100.0	130.00	70.00	0.162
38	1/25	30	0.866	3.33	0.028	100.0	170.00	70.00	0.178
39	1/25	30	0.866	3.33	0.028	100.0	200.00	70.00	0.171
40	1/25	30	0.866	3.33	0.028	100.0	230.00	70.00	0.177
41	1/25	30	0.866	3.33	0.028	100.0	250.00	70.00	0.160
42	1/25	30	0.866	3.33	0.028	100.00	130.00	80.00	0.120
43	1/25	30	0.866	3.33	0.028	100.00	200.00	80.00	0.154
44	1/25	30	0.866	3.33	0.028	100.00	230.00	80.00	0.165
45	1/25	30	0.866	5.33	0.045	100.0	130.00	30.00	0.0356
46	1/25	30	0.866	5.33	0.045	100.0	170.00	30.00	0.0319
47	1/25	30	0.866	5.33	0.045	100.0	200.00	30.00	0.006

(*continued on next page*)

Table 1 (*continued*)

Test no	m	α (°)	T (s)	H (cm)	H/L	L_X (cm)	L_G (cm)	L_B (cm)	R
48	1/25	30	0.866	5.33	0.045	100.0	130.00	50.00	0.006
49	1/25	30	0.866	5.33	0.045	100.0	170.00	50.00	0.0588
50	1/25	30	0.866	5.33	0.045	100.0	200.00	50.00	0.0224
51	1/25	30	0.866	5.33	0.045	100.0	130.00	70.00	0.0122
52	1/25	30	0.866	5.33	0.045	100.0	200.00	70.00	0.0567
53	1/25	30	0.866	3.33	0.028	133.33	133.33	40.00	0.200
54	1/25	30	0.866	3.33	0.028	133.33	266.66	40.00	0.109
55	1/25	30	0.866	3.33	0.028	133.33	133.33	66.67	0.082
56	1/25	30	0.866	3.33	0.028	133.33	200.00	66.67	0.095
57	1/25	30	0.866	3.33	0.028	133.33	226.66	66.67	0.091
58	1/25	30	0.866	3.33	0.028	133.33	266.66	66.67	0.125
59	1/25	30	0.866	3.33	0.028	133.33	306.66	66.67	0.090
60	1/25	30	0.866	3.33	0.028	133.33	333.33	66.67	0.091
61	1/25	30	0.866	3.33	0.028	133.33	386.66	66.67	0.064
62	1/25	30	0.866	3.33	0.028	133.33	133.33	93.33	0.170
63	1/25	30	0.866	3.33	0.028	133.33	266.66	93.33	0.112
64	1/25	30	0.866	3.33	0.028	166.67	166.67	83.33	0.080
65	1/25	30	0.866	3.33	0.028	166.67	283.34	83.33	0.085
66	1/25	30	0.866	3.33	0.028	166.67	333.33	83.33	0.093
67	1/25	15	0.866	3.33	0.028	100.00	100.00	50.00	0.078
68	1/25	15	0.866	3.33	0.028	100.0	130.00	50.00	0.1183
69	1/25	15	0.866	3.33	0.028	100.0	170.00	50.00	0.1133
70	1/25	15	0.866	3.33	0.028	100.0	200.00	50.00	0.1273
71	1/25	15	0.866	3.33	0.028	100.0	230.00	50.00	0.0983
72	1/25	15	0.866	3.33	0.028	100.0	260.00	50.00	0.000
73	1/25	15	0.866	5.33	0.045	100.0	130.00	50.00	−0.0079
74	1/25	15	0.866	5.33	0.045	100.0	170.00	50.00	0.0281
75	1/25	15	0.866	5.33	0.045	100.0	200.00	50.00	0.0131
76	1/25	15	0.866	5.33	0.045	100.0	230.00	50.00	−0.009
77	1/25	15	0.692	3.33	0.045	100.0	100.00	50.00	0.0264
78	1/25	15	0.692	3.33	0.045	100.0	130.00	50.00	−0.019
79	1/25	15	0.692	3.33	0.045	100.0	170.00	50.00	−0.0274
80	1/25	15	0.692	3.33	0.045	100.0	200.00	50.00	−0.0069
81	1/25	15	0.692	3.33	0.045	100.0	260.00	50.00	−0.0102

4. Numerical model studies

4.1. General

In addition to the physical model studies, numerical model studies were also performed and their results compared.

There are a number of numerical models on shoreline changes have been cited in the literature. Among them, one-line model, which considers only the shoreline change, and *n*-line model that takes into account the changes of bed contours are the most well known models. Since both cross-shore and long-shore sediment transport are dominant on a coast with T-shaped groins, three-dimensional a numerical model should be employed to compute the changes to contour. The continuity equation of

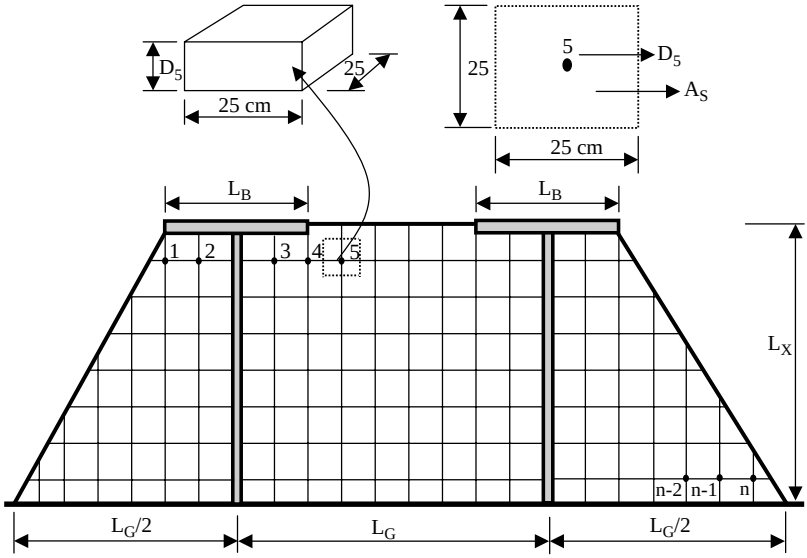


Fig. 3. Describe of the measurement.

such a model is commonly written as (Fig. 4)

$$\frac{\partial z}{\partial t} = \frac{\partial q_x}{\partial y} + \frac{\partial q_y}{\partial x} \tag{5}$$

Where t is time; q_X and q_Y are x (alongshore) and y (cross-shore) components of sediment transport discharge, and x, y and z are Cartesian coordinates.

A number of studies were performed on the point where the transport discharge is maximum, $q_X/q_{max}=1.0$. In Watanabe's equation (Watanabe, 1992, Horikawa, 1987) $0.53<x/x_b<0.85$, with an average value of $x/x_b=0.7$, where x and x_b are distances of the points of interest and breaking from shoreline, respectively. CERC equation (CERC, 1984, Hanson and Kraus, 1989) proposed that maximum transport would be at $x/x_b=0.7$.

Taking into consideration the above proposals, three kinds of models were employed in this study; $x/x_b=0$, 0.5 and 0.7, respectively.

The resulting equations for the sediment transport at these three locations are given as follows:

$$\text{For } x/x_b = 0 \Rightarrow q(x/x_b) = [1.25 - 0.7875(x/x_b)^{2/3}]Q_x \tag{6}$$

$$\text{For } x/x_b = 0.5 \Rightarrow q(x/x_b) = Q_x 11.35(x/x_b + 0.5)^{4.9}\, e^{-5x/x_b} \tag{7}$$

$$\text{For } x/x_b = 0.7 \Rightarrow q(x/x_b) = Q_x 0.98(x/x_b + 0.825)^{7.1}\, e^{-4.7x/x_b} \tag{8}$$

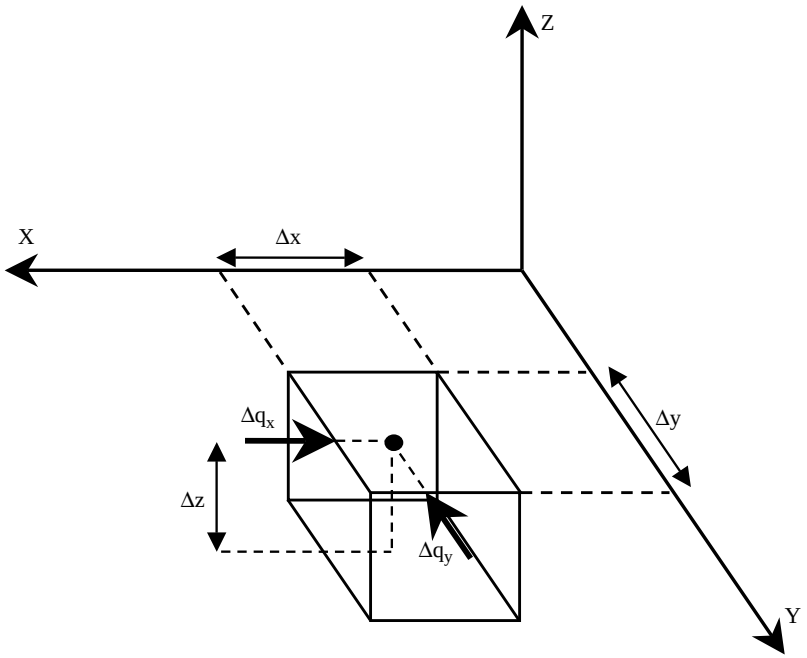


Fig. 4. Depiction of the numerical model.

In these equations, Q_x is longshore sediment transport discharge and will be explained in Section 4.2.

4.2. Sediment transport rate

There are numerous formulae to predict both cross-shore and longshore sediment transport discharges. Relevant equations used in this study are outlined.

4.2.1. Crosshore transport discharge

$$q_{\text{net}} = -1.15 \times 10^{-7} W_0 d_{50} U_{\text{r}}^{0.2} \Psi(\Psi - 0.13 U_{\text{r}}) \tag{9}$$

$$U_{\text{r}} = \frac{HL^3}{h^3}, \quad \Psi = \frac{(d_0\sigma)^2}{sgd}, \quad d_0 = \frac{H}{\sinh(2\pi h/L)}, \quad \sigma = \frac{2\pi}{T}$$

Where H, T and L are wave height, period and length, respectively, h is the depth, s, d, d_{50} mean diameter and W_0 are density, diameter and settling velocity of the sediment particle, respectively, g is acceleration due to gravity (Chiaia et al., 1995, Horikawa, 1987).

4.2.2. Longshore transport discharge

CERC formulae are as follows (CERC, 1984; Kraus and Harikai, 1983):

$$Q_x = (H^2 C_g)_b \left[a_1 \sin(2\alpha_b) - a_2 \cos(\alpha_b) \frac{\partial H}{\partial x} \right]_b \tag{10}$$

$$C_g = \left(\frac{gH_b}{\phi} \right)^{0.5}$$

$$a_1 = \frac{K_1}{[16(\gamma_s/\gamma - 1)(1-p)1.416^{2.5}]}, \quad a_2 = \frac{K_2}{[8(\gamma_s/\gamma - 1)(1-p)1.416^{2.5} \tan\beta]}$$

where α is wave angle, ϕ is the breaking index (H_b/h_b), γ and γs are specific gravity of water and sediment particles, respectively, p is porosity of sediment particles, $\tan\beta$ is bed slope, K_1 and K_2 are empirical coefficients ($0.58 \le K_1 \le 0.77$, $0.5K_1 \le K_2 \le K_1$) and subscript b denotes wave breaking point.

Kamphuis (Kamphuis, 1991) proposes a different formula:

$$Q = 0.00203 H_b^2 T^{1.5} m^{0.75} d_{50}^{-0.25} \sin^{06}(2\alpha_b) \tag{11}$$

Where H, T, and α are wave height, period and angle, respectively, m is bed slope, d_{50} mean diameter and subscript b denotes wave breaking point.

4.3. Execution of the numerical model

By using Eqs. (5)–(10), a numerical scheme was developed to compute the bed changes. The studied area was divided into 12.5×12.5 cm grids. Positive directions of Q_X (longshore) and Q_Y (cross-shore) values are given in Fig. 5. Wave breaking height in the model was computed by (CERC, 1984):

$$K = b - a\frac{H_b}{gT^2}, \qquad H_b = Kh_b, \quad a = 43.75(1 - e^{-19m}), \quad b = \frac{1.56}{(1 + e^{-19.5m})} \tag{12}$$

Where m is the bed slope ($=\tan\beta$).

Shoaling (K_s) and refraction (K_r) coefficients were calculated by assuming shore parallel straight bed contours. In calculating diffraction coefficient (K_D) at the gap of two T-shaped groins, K_D values of each groin were multiplied.

5. Field study

The field study was carried out at two locations at Of (a town 50 km east of Trabzon Province) Coast in which there were a T groin field with two groins and a single T groin (Karasu, 1998).

Coast with one T Groin: There is a single T groin with 60 m length and 40 m head length. At the beginning of the measurements, the bed contours were roughly straight

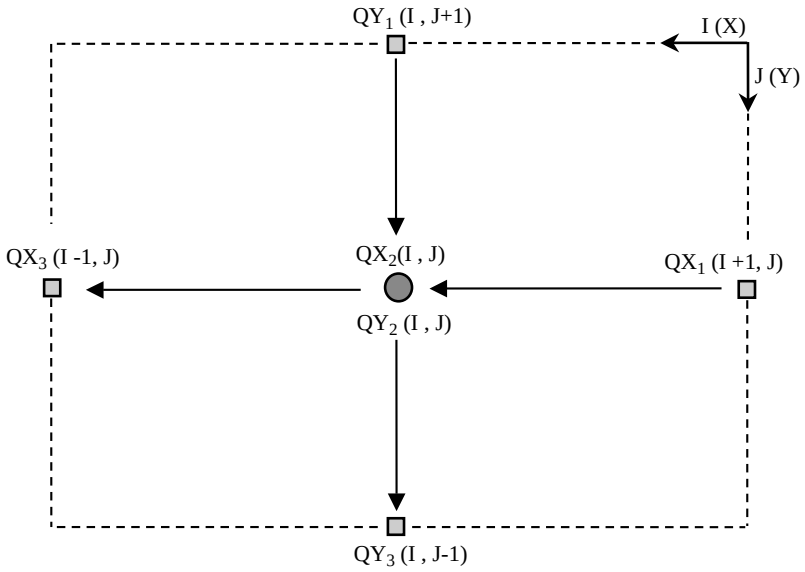


Fig. 5. Positive directions of sediment transport in the numerical model.

and parallel to the shoreline; the depth at the outer part of the head was 2 m, which means that the average bed slope was 1/30. The bed contours, measured 6 months later from construction, are given in Fig. 6. The resulting bed contours of the numerical model are presented in Fig. 7.

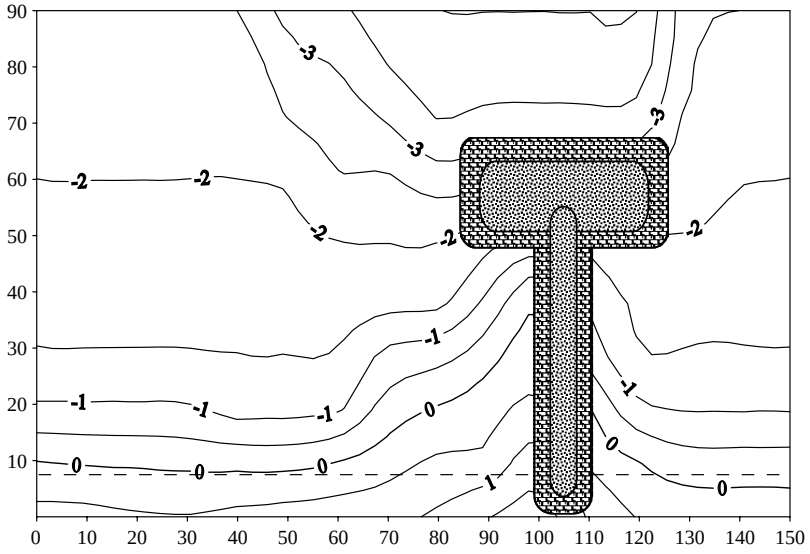


Fig. 6. The bed topography of one T Groin (Field study, 6 months later from construction).

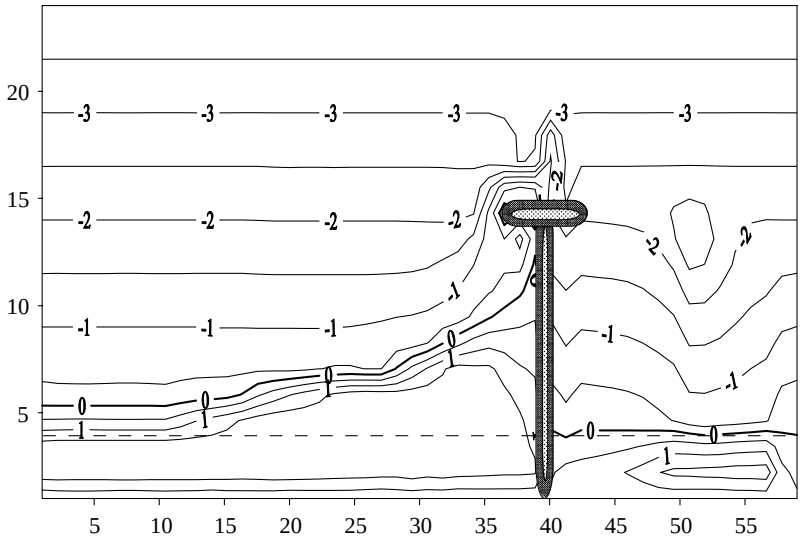


Fig. 7. The bed topography of one T Groin (Numerical model, 6 months later from construction).

Coast with T Groin Field (two T Groins): There are two T groins with the same dimensions and bed topography as the above one T groin. The bed contours measured 6 months later from construction and obtained from numerical model are presented in Figs. 8 and 9, respectively.

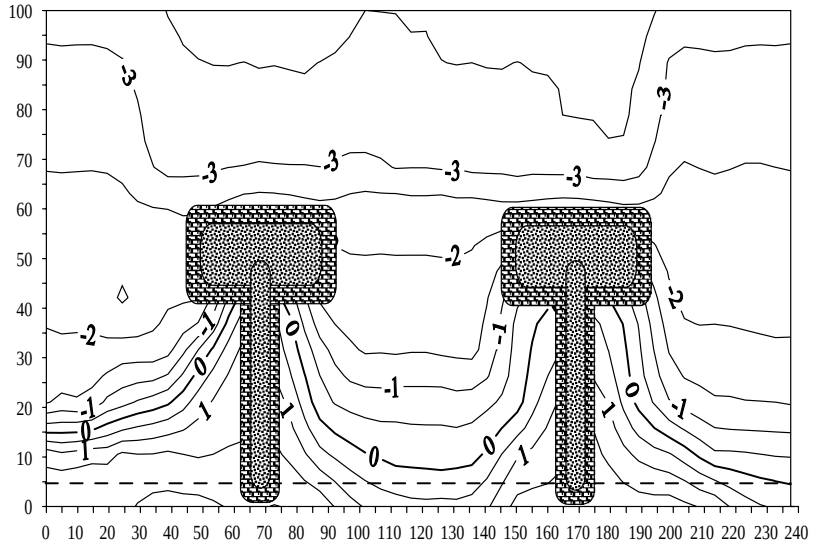


Fig. 8. The bed topography of T Groin Field (Field study, 6 months later from construction).

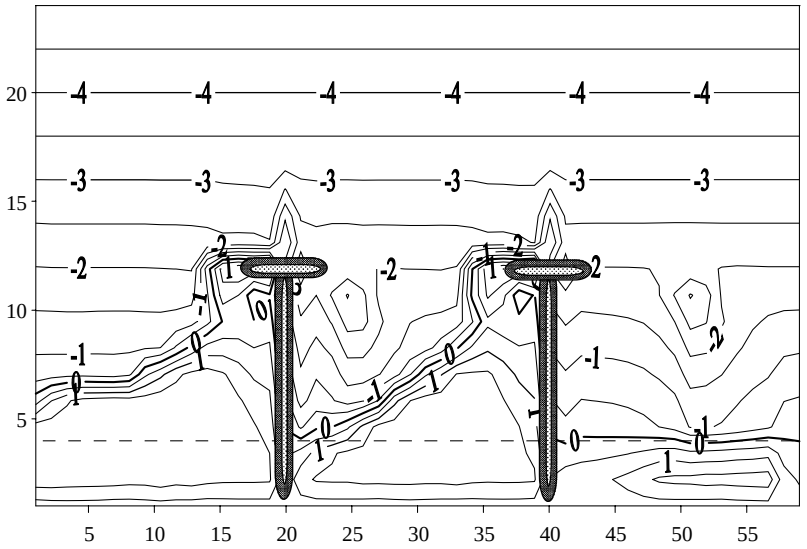


Fig. 9. The bed topography of T Groin Field (Numerical model, 6 months later from construction).

6. Evaluation of physical model results

In this section, the effects of various groin and wave parameters on the dimensionless accretion parameter (R) are discussed.

6.1. Effect of groin length (L_X)

In order to study the effect of groin length on the accretion parameter; totally 12 experiments were performed. In these experiments; H, T, and L_B/L_X were kept constant as 3.33 cm, 0.866 s, and 0.5, respectively. Then four L_X values (66.7, 100, 133.3 and 166.7) were chosen and for every L_X values, three experiments were conducted by changing L_G/L_X values (1, 1.7 and 2). The results are given in Fig. 10.

As seen from Fig. 10, for all groin opening, as the groin length is 100 cm, the greatest amount of accretion (R) are obtained. Initially, R values are increasing from groin length of 66.66–100 cm and after 100 cm of groin length, it has been decreased. It is clear that the amount of accretion decreases with the groin opening increase.

6.2. Effect of groin opening (L_G)

The results of the experiments that were carried out to study the effect of L_G on R are given in Figs. 11 and 12. As can be seen, maximum R values are obtained when $L_G/L_X \cong 2.0$. All three lines in Fig. 11 have similar tendency. Among these lines, R values is maximum at $L_X = 100$ cm.

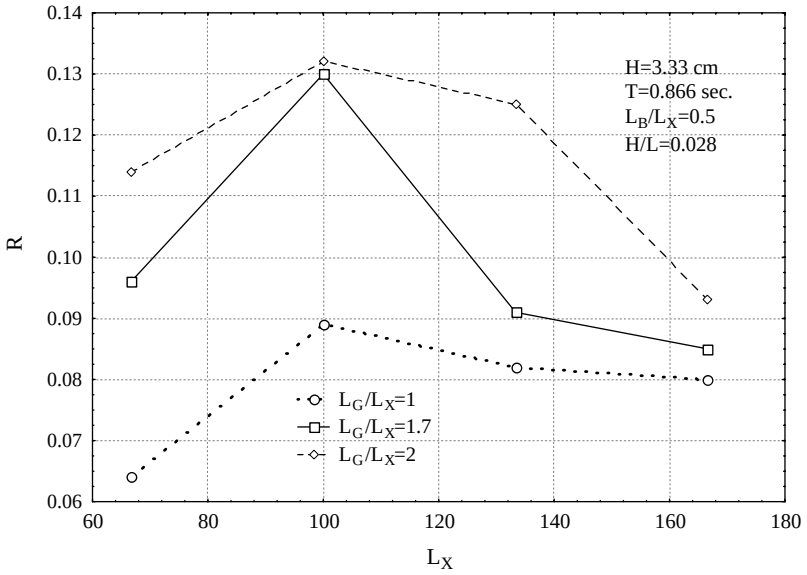


Fig. 10. The effects of groin length on accretion for various groin gaps ($\alpha = 30°$).

6.3. Effect of head length of groin (L_B)

The results of the experiments which were performed to study the effect of L_B on R are given in Figs. 12 and 13. In Fig. 12, for three values of L_B/L_X (0.3, 0.5 and 0.7),

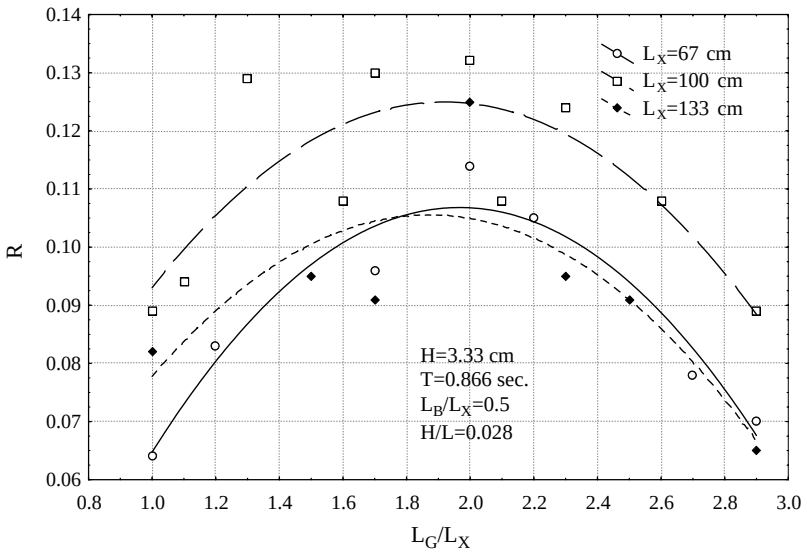


Fig. 11. The effects of groin length on accretion for various groin lengths ($\alpha = 30°$).

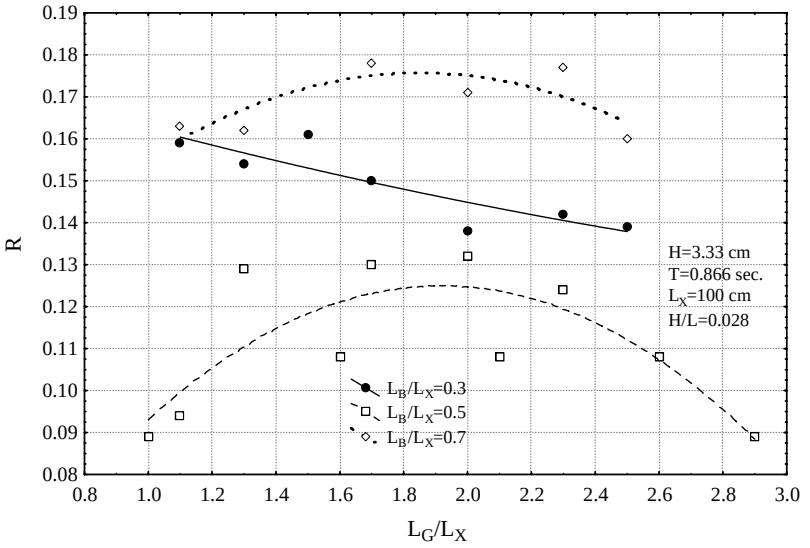


Fig. 12. The variation of R vs. L_G/L_X.

the variation of R depending on L_G/L_X is given. As can be seen, maximum R values are obtained in the case of $L_B/L_X = 0.7$. In Fig. 8, the variation of R by L_B/L_X is plotted for various L_G/L_X values. The general trend of the scattering points results in that an increase in L_B/L_X give rise to an increase in R values. Consequently, it is obvious that, the longer

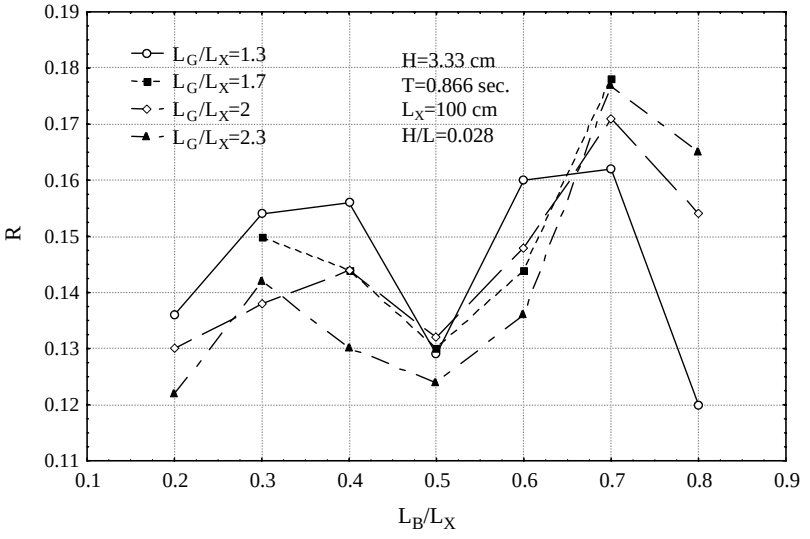


Fig. 13. The variation of R vs. L_B/L_X.

head the more accretion. However, this will cause more expensive structures. A benefit–cost analysis should be carried out to obtain the optimum solution.

6.4. Effect of wave height (H)

The experimental results given in Figs. 14 and 15 which describe the effect of H on R imply that if H goes up, R values will lessen.

6.5. Effect of wave period (T)

By analysing the experimental results presented in Fig. 15, it can be easily seen that, an increase in T values causes an increase in R values. In other world, the less steep waves, the more accretion.

6.6. Effect of wave angle (α)

The experimental results for $\alpha = 30$ and 15° are presented in Figs. 16 and 17, respectively. It is obvious that, more R values are observed in the case of $\alpha = 30°$. This case is more clearly for $H = 5{,}33$ cm value.

7. Evaluation of numerical model results

Numerical model were performed according to CERC Model for $x/x_b = 0$, 0.5 and 0.7; and to Kamphuis Model for $x/x_b = 0$ (Hanson and Kraus, 1989; Kamphuis, 1991).

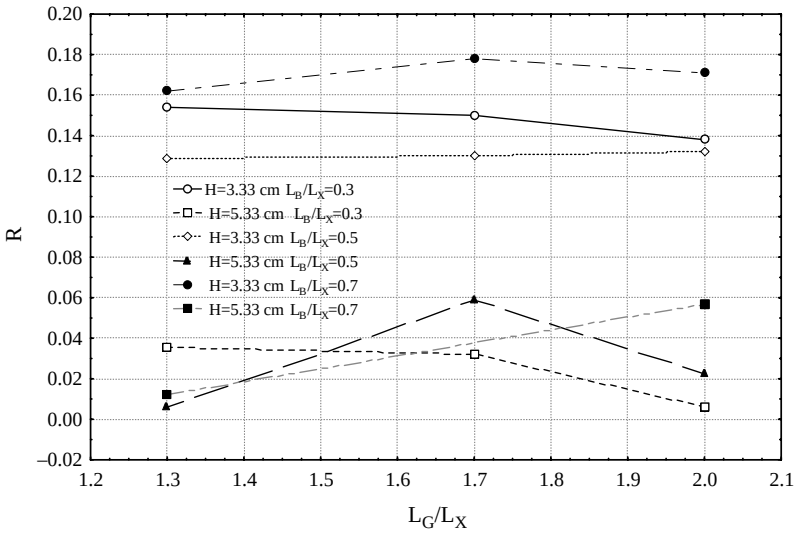


Fig. 14. The effects of wave height on accretion ($\alpha = 30°$).

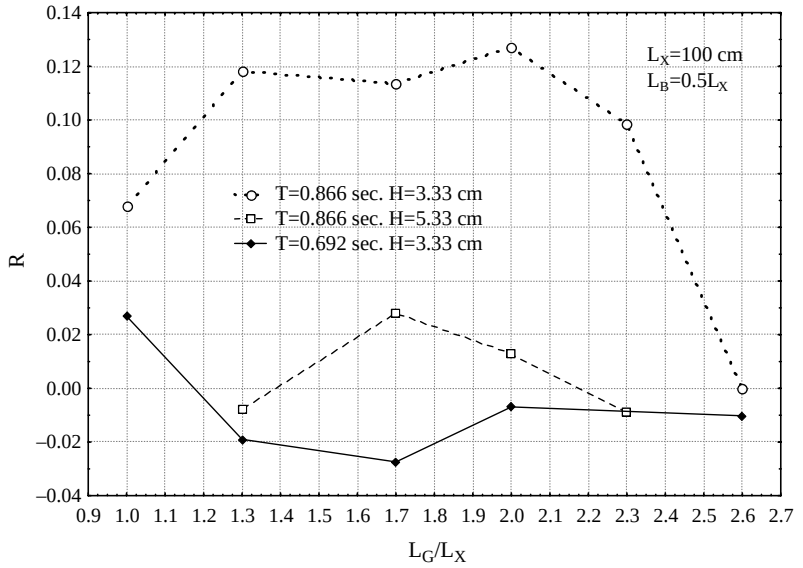


Fig. 15. The effects of wave period on accretion for various groin lengths ($\alpha = 30°$).

The results of these four models are presented in Fig. 18, in which the variation of R versus L_G/L_X was plotted for constant values of $H = 3.33$ cm, $T = 0.866$ s. and $\alpha = 30°$. It can be seen that, the greatest R values are obtained by both Kamphuis model and CERC model for $x/x_b = 0$ and their results are similar. CERC model for $x/x_b = 0.5$ and 0.7 result in relatively small and near R values.

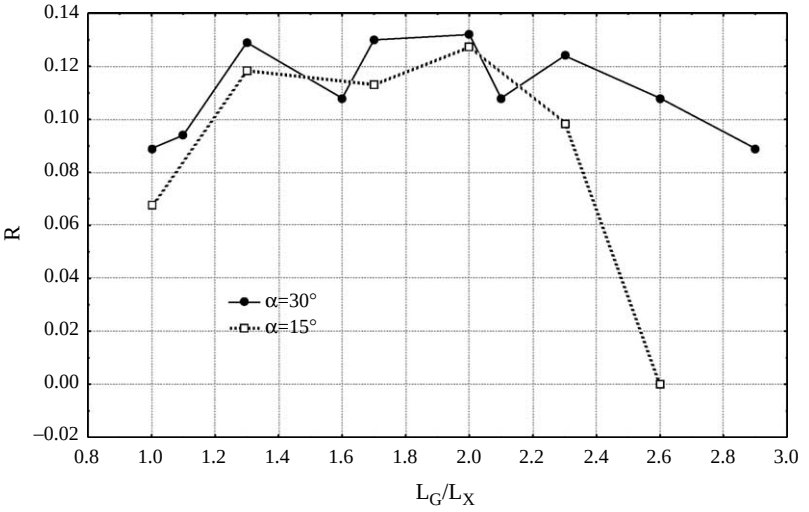


Fig. 16. The effects of wave angle on accretion ($H = 3.33$ cm).

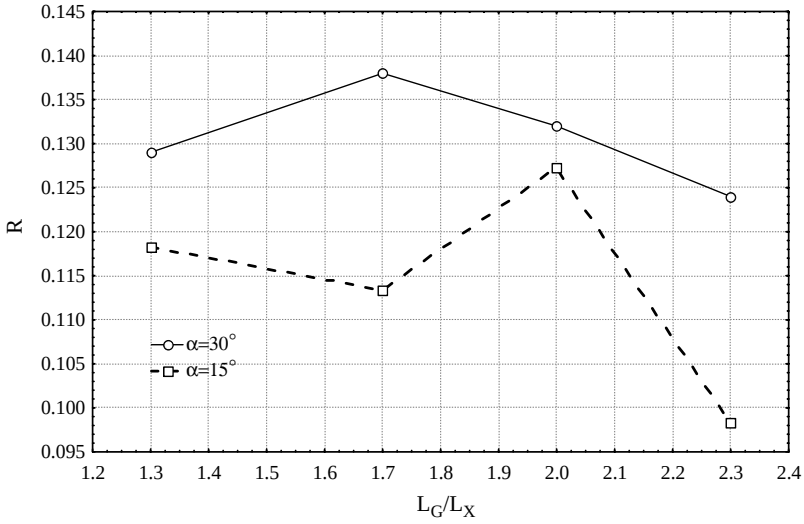


Fig. 17. The effects of wave angle on accretion ($H=5.33$ cm).

By comparing the results of physical and numerical models carried out at the same conditions, it was concluded that, the nearest results between two models were observed by CERC model for $x/x_b=0$. Therefore, in the following analyses, only the results of this model are employed.

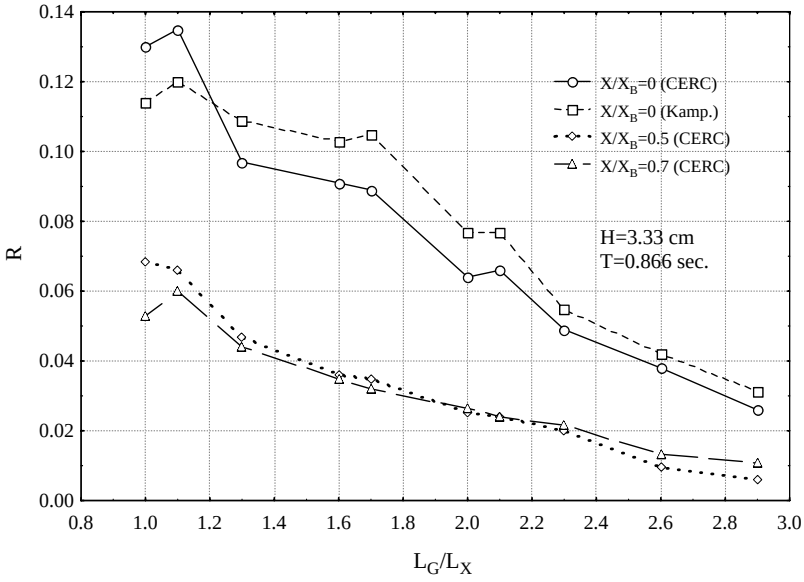


Fig. 18. The results of the tested numerical models ($\alpha=30°$).

It can be seen from Fig. 18 that, the smaller L_G/L_X, the smaller R values. These results disagree with physical model results which yield the maximum R values in the case of $L_G/L_X \cong 2.0$ (Figs. 11 and 12).

The results of the physical and the numerical models are given in Fig. 19. It is obvious that, the R values of the physical models are greater than those of numerical models.

8. Analysis of the field study results

The results of the numerical model and field measurement of R values for one T groin and for T groin field are given in Figs. 20 and 21, respectively.

8.1. Analysis of bed topography changes

As can be seen from Figs. 6 and 7, one groin caused remarkable accretion at the updrift (west) side and some erosion at the downdrift (east) side of the groin. Some erosion has been observed at the head zone of the groin. The field measurements have yielded less accretion than that of the numerical model. The erosion patterns of the measurements and numerical model are similar.

8.2. Analysis of the results of dimensionless accretion parameter

In the case of one groin (Fig. 20), the dimensionless accretion parameter (R) has similar characteristics both in field and numerical model. During the winter season (from

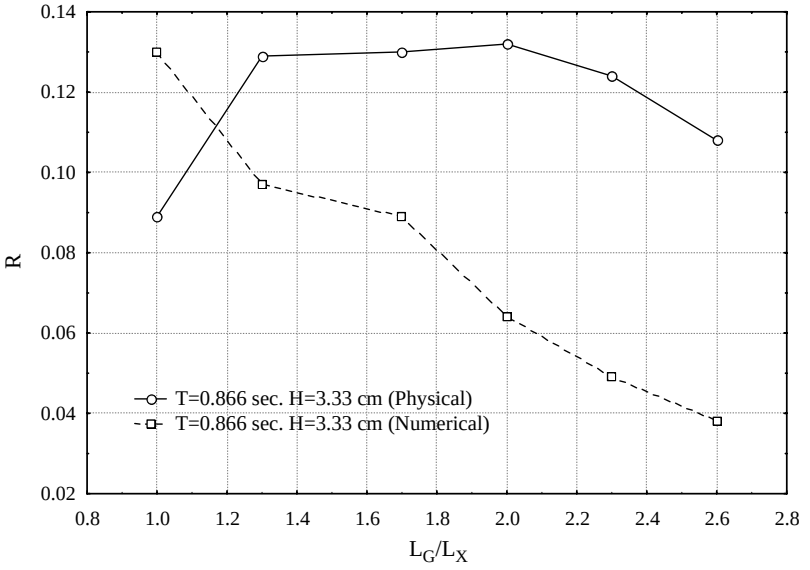


Fig. 19. The results of the physical and the numerical models.

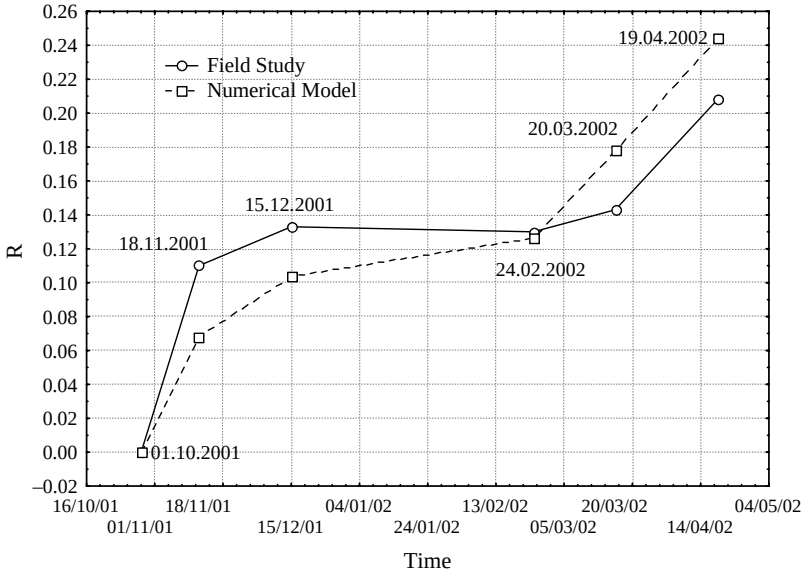


Fig. 20. The variation of R with time (one T Groin).

November to February), there is no increase in R values in measurements, mainly due to steep waves that caused offshore sediment transport.

In the case of groin field (Fig. 21), remarkable accretion has been observed in nature. The numerical model, however, has yielded less accretion.

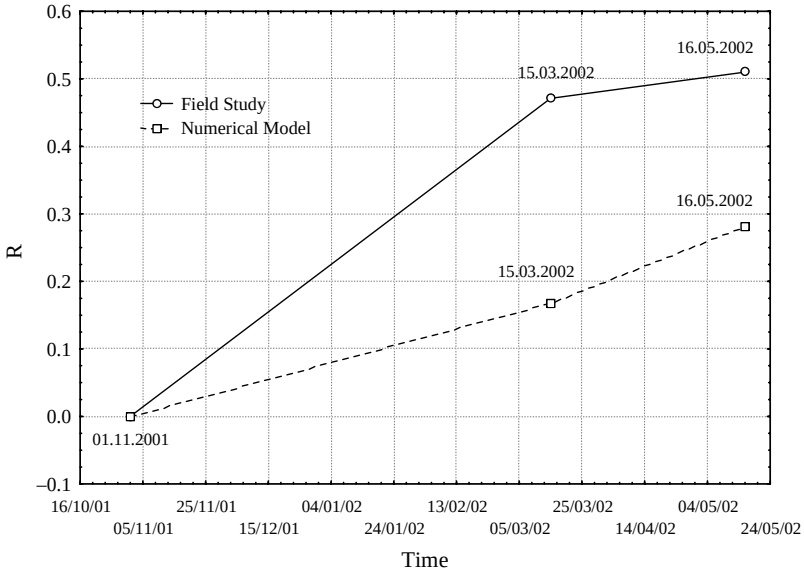


Fig. 21. The variation of R with time (T Groin Field).

By comparing Figs. 20 and 21, since groin field has yielded greater R values than one groin, it is obvious that, a groin field is more effective than one groin.

9. Conclusions

In this study, the effect of various groin parameters (length, head length and opening) and wave parameters (wave height, wave period and wave angle) on the dimensionless accretion parameter R of a region which is protected by T shaped groins are studied by both physical and numerical models. The results of a numerical model are compared with field data that were obtained by deep sounding measurements at Of coasts, Trabzon Province, Turkey. The conclusions of this study may be summarised as follows:

For all groin opening, as the groin length is 100 cm, the greatest amount of accretion (R) are obtained. After 100 cm of groin length, it has been decreased in R. However, this does not result in a decrease in total accretion volume; because of the fact that, L_X also affect the total protection area and consequently, R.

In order to get more accretion, the head length of groin should be as long as possible, and, in order to find the optimum head length, taking into consideration of local conditions, and a benefit–cost analysis should be performed.

According to the results of physical model studies, maximum R is obtained when the ratio of the opening between two successive groins to the groin length (L_G/L_X) is equal near to two ($L_G/L_X \cong 2.0$), however, this opinion is not supported by the results of numerical model, which implies that the smaller L_G/L_X, the smaller R. Since the physical models are more reliable than numerical models (because of more assumptions in the latter), it is recommended that L_G/L_X be nearly equal to two.

In the case of greater values both of wave period and angle, greater accretion are expected and this conclusion was supported both by physical and numerical model results.

According to the experimental results, H values goes up, R values will lessen. In addition, numerical model results are opposite the experimental results. If it is look over the text, it is clear that the amount of discharge (Q) increases with H value increase. However, this case has not been erosion on the beach. Amount of accretion is dependent on both the breaking wave whether or not is in the protecting area, and winter profile which is formed with greater H value on beach.

Monochromatic waves were reproduced in the model, which resulted in a uniform breaking zone. In nature, spectral wave conditions, with a varying breaker zone along the shoreline, are more representative. During the physical studies, the scale was chosen based on laboratory space and available measuring equipment. Sediment scaling relations have not yet been developed to accurately measure the quantitative movement of sediment.

The aforementioned stipulations of course, affect the reliability of the results. But, since some conclusions obtained from various studies related to this study are in agreement with these conclusions, it is possible to say the results are useful in planning the preliminary layout for T groins. However, more comprehensive field and/or laboratory studies should be conducted relative to this problem, prior to final design of T groins.

The numerical model, used in the prediction of bed topography changes in the vicinity of groins, has resulted in similar characteristics as field measurements.

A groin field with two T groins is more effective than one T groin, both in coastal protection and in extension of beaches.

In order to reach more reliable conclusions, more field data are necessary.

References

Brampton, A.H., Goldberg, D.G., 1991. Mathematical Model of Groins on Shingle Beaches, Report SR 276, Hydraulics Research Ltd., Wallingford, Oxfordshire OX10 8BA, United Kingdom, November.

Brampton, A.H., Goldberg, D.G., 1991b. Mathematical model of groyned shingle beaches Coastal Sediments'91, vol. 2 1991 pp. 1842–1853.

CERC, 1984.Anon., 1984. Shore Protection Manuel, fourth ed. US Army WES, Washington.

Chiaia, G., Damania, L., Petrillo, A., 1995. Analysis of Cross-Shore Transport International Conference on Coastal and Port Engineering in Developing Countries, Brazil 1995 pp. 412–426.

Güngördü, Ö., Otay, E.N., 1997. Numerical Model of Shore Change, Advances on Civil Engineering 3th Technical Congress. METU, Ankara, Turkey pp. 701–710 (In Turkish).

Hanson, H., Kraus, N.C., 1989. GENESIS: Generalized Model for Simulating Shoreline Change, Report 1, Technical Reference. CERC, Mississippi pp. 25–57.

Hanson, H., Kraus, N.C., 1991. Comparison of Shoreline Change With Physical and Numerical Models Coastal Sediment'91, vol. 1. ASCE, New York pp. 1785–1799.

Horikawa, K., 1987. Nearshore Dynamics and Coastal Processes. University of Tokyo Press, Tokyo, Japan.

Kamphuis, W.J., 1991. Alongshore sediment transport rate. Journal of Waterway, Port, Coastal and Ocean Engineering, ASCE 117 (6), 624–640.

Karasu, S., 1998. The Effects of Groins on the Black Sea Coast and A numerical Model Approach, MsC Thesis, Institute of Natural and Applied Sciences, KTU, Trabzon, Turkey (In Turkish).

Kraus, N.C., Harikai, S., 1983. Numerical model of the shore line change at Oarai beach. Coastal Engineering 7, 1–28.

Kraus, N.C., Hanson, H., Blomgren, S.H., 1994. Modern Functional Design of Groin System. Coastal Engineering, 1327–1342.

Leont'yev, I.O., 1997. Short-term shoreline changes due to cross-shore structures: a one line numerical model. Coastal Engineering 31, 59–75.

Moutzouris, C.I., 1992. Observation of the Post-Construction Performance of a System of Groins Along on Eroding Beach Coastal Engineering Practice'92. Long Beach, California pp. 303–319.

Özölçer, I.H., 1998. A Study on the Effects of Groins in Shore Protection, PhD Thesis, Institute of Natural and Applied Sciences, KTU, Trabzon, Turkey (In Turkish).

Press, H., 1962. Seewosserstrakenundseehafen, Verlagvon Wilhelm Ernst und Sohn, Berlin-München 1962 pp. 814–864.

Price, W.A., Tomlinson, K.W., 1968. The effect of groins on stable beaches. Coastal Engineering 1, 518–526.

Watanabe, A., 1992. Total rate and distribution of long shore sand transport. Coastal Engineering, 2528–2544.

Yüksek, Ö., 1995. Effects of breakwater parameters on shoaling of fishery harbors. Journal of Waterway, Port, Coastal and Ocean Engineering 121 (1), 13–22.

Yüksek, Ö., Kömürcü, M.I., Tokgöz, A., 1999. Determination of Coastline Changes in Black Sea, Tenth Engineering Symposium Proceedings on Civil Engineering. Süleyman Demirel University, Isparta, Turkey pp. 81–91 (In Turkish).